Microfluidics and Nanofluidics (2022) 26: 66
https://doi.org/10.1007/s10404-022-02556-w

RESEARCH PAPER

RF sensor-based tracking of nanoparticle's morphological and relative arrangement variations

Annesha Mazumder[1] · Tapan K. Sau[2] · Syed Azeemuddin[1] · Prabhakar Bhimalapuran[2]

Received: 18 September 2021 / Accepted: 20 May 2022 / Published online: 6 August 2022

Abstract

This article explores the feasibility of utilizing an interdigitated capacitor (IDC) based RF sensor for studying nanoparticle properties. The parameters include their size, shape, thickness, and relative arrangement in aqueous media. The analysis is carried out using the CAD tool high frequency structure simulator (HFSS). We study the variation in properties of spherical, cubical, disc-shaped, and polyhedral gold nanoparticles. The change in the resonance frequency, resonance amplitude, and − 3 dB bandwidth is analyzed for each case. The findings show that the change in the IDC-based RF sensor's resonance characteristics can be used to track the variations in morphology and arrangements of gold nanoparticles.

Keywords Sensing · Radio frequency · Gold nanoparticles · RF sensing

1 Introduction

The sensing market has exponentially grown in the last couple of decades. The idea has been to develop fast and facile sensors capable of efficiently delivering results without sophisticated instrumentation. However, most conventional techniques have fallen short due to their cumbersome, time-taking and labor-intensive procedures. They require several rounds of incubation and washing. Further, most of them can not be conducted outside of laboratories. Additionally, they are often not reusable and require expensive fabrication and synthesis methods. There is, thus, a need to explore possible alternatives that can tackle the challenges faced by traditional techniques.

Among the various methods currently being investigated, radio frequency based sensing has emerged as a suitable alternative (Mehrotra et al. 2019; Lee and Yook 2014; RoyChoudhury et al. 2016). RF sensing offers fast and facile solutions. It involves highly simplified procedures for both sample preparation and testing. Most of these techniques are also label-free. The need for sophisticated instrumentation and lab facilities is reduced for these methods. These procedures are usually not labor-intensive. Furthermore, they typically require minute volumes of liquids for analysis. These RF sensors can also be easily fabricated and integrated with existing IC technology.

These sensors study the interaction of matter with EM waves. The response of the sensor changes in the presence of different samples due to the unique interactions between the EM waves and the sample. They study the variation in different electrical and magnetic quantities such as permittivity, permeability and conductivity. Subsequently, the variation in these parameters is mapped to perform qualitative and quantitative analysis. Popular RF sensors include coplanar waveguides (Shete et al. 2013; Chen et al. 2014; Mohammadi et al. 2020; Xu et al. 2019) interdigitated capacitors (Kim 2008; Rukavina 2015), split ring resonators (Boybay and Ramahi 2012; Velez et al. 2017) and patch antennas.

RF-based sensors have been employed for myriad applications in the recent past. Biomedical and biochemical areas have especially drawn much interest. The most popular applications of RF sensing are in the detection of biomolecules and pathogens (Elsheakh et al. 2013; Narang et al. 2018; Jang et al. 2006; Lee et al. 2012; Bahar et al. 2019; Xu 2021; Kim et al. 2008). They deliver results

✉ Syed Azeemuddin
syed@iiit.ac.in

✉ Prabhakar Bhimalapuran
prabhakar.b@iiit.ac.in

[1] Center for VLSI and Embedded Systems Technologies, International Institute of Information Technology, Hyderabad 500032, India

[2] Center for Computational Natural Sciences and Bioinformatics, International Institute of Information Technology, Hyderabad 500032, India

rapidly and can be easily put into use without the requirement of well-equipped laboratories. This makes them an excellent candidate for performing diagnostic tests. RF based sensors have also shown promising results in performing physiological as well as pathological analysis of cells (Nikolic-Jaric et al. 2009; Grenier et al. 2010; Zhang et al. 2012; Peyman et al. 2015; Surowiec et al. 1988; Wu 2016; Dalmay et al. 2014). In particular, they have shown great potential in performing differentiation of tumor cells from healthy cells. They have also been utilized in identifying the stage and type of cancer (Zhang et al. 2012; Peyman et al. 2015; Surowiec et al. 1988; Wu 2016). The other widespread use of RF based sensing is in dielectric spectroscopy, especially for the analysis of bioliquids (Nee Haase et al. 2015; Facer et al. 2001; Mateu et al. 2007; Booth et al. 2010; Song et al. 2006; Ocket et al. 2013).

In recent times, nanoparticle-based sensing has also become immensely popular. They are used in a plethora of applications, including biochemical and biomedical domains. Their widespread popularity could be attributed to the unique properties exhibited by them. At the nanoscale, materials exhibit properties dramatically different from their bulk counterparts (Rotello 2004; Daniel and Astruc 2004; Schmid 2011). The properties of the nanoparticles can be tuned by synthesizing controlled sized, and shaped nanoparticles (Grzelczak et al. 2008; Jana et al. 2001; Sau and Murphy 2004). These have been exploited to track the target species' absence, presence, variation or their bindings near the nanomaterials. They have been utilized for a wide range of sensing applications, including the detection and identification of biomolecules, pathogens and toxins (De et al. 2008; Baetke et al. 2015; Han et al. 2019; Zazo et al. 2016). It will be of paramount importance to employ RF-based sensing to detect the variations in the nanoparticle's features like the morphology and arrangement, which control nanoparticle's properties (Mazumder et al. 2020a, b).

Plasmonic nanoparticles form an important part of nanoscience. These plasmonic nanoparticles consist of metallic nanoparticles such as Au, Ag and Pt nanoparticles. They have unique optical properties and are frequently used in detection (Yue et al. 2016; Wang et al. 2017; Liu et al. 2018; Wang et al. 2018; Chang et al. 2017; Wu et al. 2017; Zou et al. 2018; Haes et al. 2004; Dondapati et al. 2010; Hong et al. 2012; Su et al. 2014; Wang et al. 2010). In particular, they participate in a distinctive optical phenomenon known as localized surface plasmon resonance.The wavelength at which the maximum absorption takes place depends on several interlinked factors. This includes the nature of the metal used, the nanoparticle's shape, size and configuration as well as the properties of the material used to functionalize the surface. The λ_{max} peak can be very carefully tuned for highly specific applications and this enables the widespread use of nanoparticles in the sensing industry. Detection is performed based on the shift observed in the λ_{max} peak.

In this study, we assess the potential of using simple and rapid RF-based sensing for studying the variation in the morphological parameters and relative arrangements of nanoparticles in aqueous media. This work performs an extension of the analysis carried out in Mazumder et al. (2020a) where disc-shaped gold nanoparticles were studied. It carries out detailed analyses with spherical, cubical, and polyhedral gold nanoparticles. We have utilized an interdigitated capacitor based RF sensor resonating at 60.95 GHz to perform the analysis of the variation of different features of gold nanoparticles. We have employed the high-frequency structure simulator (HFSS) for the study. The study was based on determining the changes in the S_{11} parameter due to the variation of the nanoparticle features. We have determined the resulting changes in the resonance frequency, resonance amplitude, and − 3 dB bandwidth. In the following, we discuss these resonance results as a function of particle parameters like the radius, thickness, shape, and relative arrangement of gold nanoparticles.

2 Materials and methods

In this section, we first discuss the design of the sensor being utilized. Next, the preparation methodologies for all the samples under test are discussed in details (Fig. 1).

2.1 Sensor design

We have performed the analysis using high-frequency structure simulator (HFSS) for a IDC based RF sensor. IDCs are

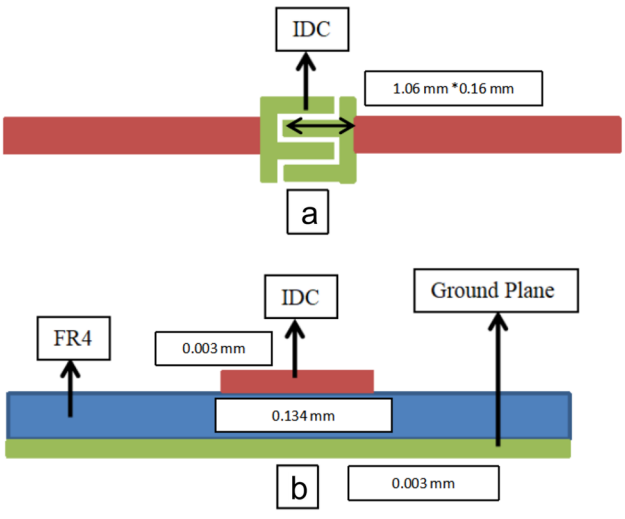

Fig. 1 **a** Top-view of IDC based RF sensor and **b** side-view of IDC based RF sensor

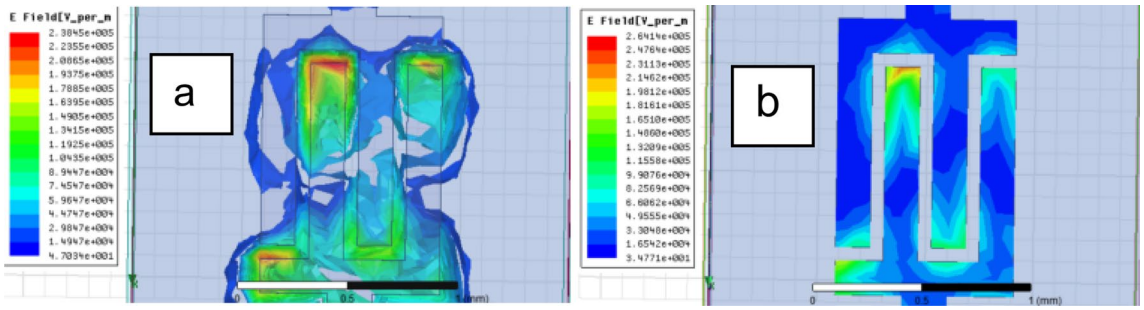

Fig. 2 E-Field of IDC based RF sensor in air: **a** between finger and **b** on top of fingers

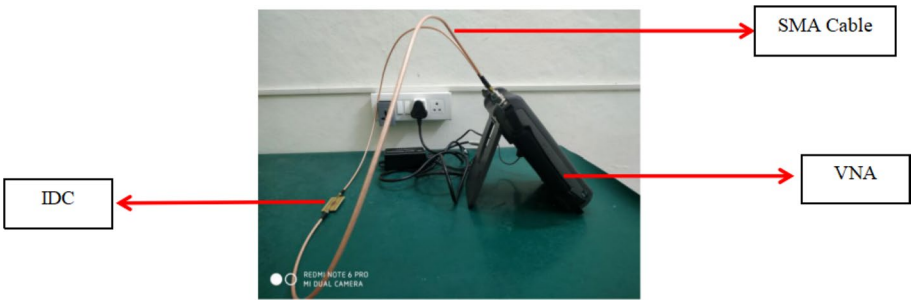

Fig. 3 Experimental setup with fabricated IDC

facile structures that are associated with simple design and fabrication process. They are also light-weight and can be easily integrated with existing IC technology. The sensor is designed to operate at 66.76 GHz. It comprises four fingers of length 1.06 mm and width 0.16 mm, with finger spacing of 0.063 mm. The sensor is built on top of a 0.134 mm thick FR4 substrate. The ground plane as well as the metallic design on top is built from 0.003 mm thick Cu. The Cu layer is coated with an insulating material to avoid direct interaction of the metallic design and the sample. In the presence of water, a frequency shift of 10.96 GHz is obtained. The sensitivity of the IDC based sensor can be estimated to be 0.137, where the sensitivity is defined as

$$\text{Sensitivity (S)} = \delta f / \delta \varepsilon \tag{1}$$

The E-Field distribution has been shown in Fig. 2. The maximum E-Field is present between the fingers and on the fingers. The E-Field lines that begin on the IDC reach the ground plane either through the substrate or in the form of fringing fields.The sample is kept on top of the insulating layer. In the presence of the insulating layer and the sample, the net permittivity of the medium through which the fringing fields reach the ground plane changes. This results in a variation in the resonance characteristics of the sensor in the presence of different samples.

We have particularly analyzed spherical, cubical, and polyhedral gold nanoparticles along with gold particles coated with biolayer as samples. For each analysis, a group of thirty gold nanoparticles was taken and immersed in the water layer.

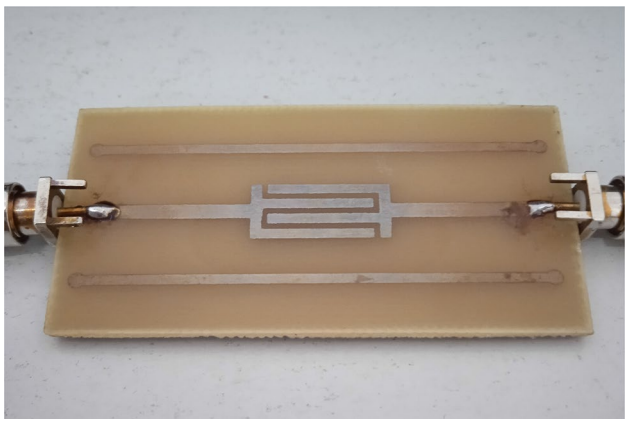

Fig. 4 Fabricated IDC resonating at 5 GHz

2.1.1 Fabrication and experimental setup

The IDC based sensor that resonates at 5 GHz is fabricated (Porwal et al. 2016). The interdigitated structure has four fingers, each 12.7 mm long and 1.9 mm wide, with a gap of 0.76 mm between them. The sensor is fabricated on a 1.6 mm thick FR4 substrate with a 0.035 mm copper layer on top. The sensor is connected to an Agilent VNA of 6 GHz to measure the frequency response using s-parameters, specifically the reflection coefficient (Figs. 3, 4). The response

changes in the presence of different analytes and is used to perform the differentiation.

The dimensions of the fabricated sensor don't match with the simulated one due to fabrication limitations.

2.2 Gold nanosphere synthesis and conjugation with BSA

The Gold Nanospheres are synthesized using a seed-mediated process. The methodology involves two major steps- (i) the synthesis of small seed particles and (ii) the development of the required gold nanospheres using the seed prepared in (i).

I. Preparation of seed solution

In order to prepare the seed solution, CTAB solution and $NaBH_4$ solution, is first prepared. 0.1 M CTAB solution is prepared by dissolving the required amount of CTAB in millipore water and mixing it using a magnetic stirrer. The CTAB solution can't be more than 30 days old for the GNSP synthesis. 0.01 M of $NaBH_4$ solution is prepared next by adding $NaBH_4$ to cooled millipore water. The solution is thoroughly mixed with the help of the vortex machine. The vessel containing the solution is then placed in a suitable environment to avoid any change in temperature of the $NaBH_4$ solution. The $NaBH_4$ solution should be freshly prepared to ensure the correct formation of seed.

The seed solution is prepared using ice-cold Sodium borohydride ($NaBH_4$) solution as the reducing agent, solution as the gold precursor and CTAB as the capping agent. 3 ml of 0.1 M CTAB is first added to millipore water and then 100 µl of the gold precursor, $HAuCl_4$ solution, is added to the mixture. The solution is a bright golden yellow at this stage. After this, 240 µl the ice-cold $NaBH_4$ solution is added carefully, and the colour of the solution changes to brown. After the addition of each reagent, the solution is first mixed with the help of inversion mixing and then using a Vortex machine. This is essential to ensure that the mixing has taken place uniformly. The seed solution is allowed to settle for at least 2 h before being used for making the gold spheres.

II. Preparation of GNSP from seed solution

The GNSP growth solution is prepared using Ascorbic Acid (AA) as a reducing agent, CTAB as the capping agent and $HAuCl_4$ as the precursor. 5 ml of 0.1 M AA solution is freshly prepared by adding the required amount of AA to millipore water. To prepare 10 ml of gold nanospheres, 160 µl of 0.1 CTAB solution is added to 9.0352 ml of millipore water and mixed. 200 µl of $HAuCl_4$ is added next which turns the solution golden yellow. Upon adding 600 µl of AA, the solution turns colourless due to the reduction of Au^{3+} ions. 4.8 µl of seed solution is carefully added at the end. After mixing the solution using the vortex machine, it starts turning pink. It attains a bright wine red colour after some time. It has to be kept for at least 6 h before being taken for centrifugation. The GNSP are centrifuged at 10,000 r.p.m for 15 min. The residue is preserved while the supernatant is thrown away.

10^{-6} M solution of BSA in PBS Buffer of pH 6.8 is prepared and the gold residue from the previous step is added to it. The sample is allowed to settle for 20 minutes, after which the reading is taken for the GNSP-BSA conjugate in PBS Buffer. For the GNSP in PBS sample also, the residue is allowed to settle in PBS Buffer of pH 6.8, before being taken for testing.

3 Results

In the following, we discuss the effect of the variation of different physical parameters of gold particles and relative arrangements of gold particles on the sensor's resonance characteristics. The resonance characteristics involve the resonance frequency, resonance amplitude, and − 3 dB bandwidth. Most of the RF sensing studies use the change in the resonance frequency for the sample analysis. The resonance amplitude parameter has also been used in some cases. Along with these, in this work, we have explored the − 3 dB bandwidth parameter variation. The idea is to build a comprehensive understanding of the various parameters and characteristics that will help to obtain unique sensing signatures for different samples.

3.1 Simulation based study: variation of morphological features of gold particles

In Mazumder et al. (2020a), the properties of disc-shaped gold particle were analyzed. It was shown that as the radius of the disc-shaped particle increases, the resonance frequency increases. Further analysis showed that an increase in the thickness of the disc-shaped particle is also associated increase in the resonance frequency.

In this work, we extended the analysis of variation of physical properties to other shapes. We have varied the physical properties of cubical gold particles, spherical gold particles and polyhedral gold particles. For each of these analyses, a group of thirty gold particles is taken and immersed in the water layer. For each case, the analysis studies the change in the resonance characteristics in terms of the resonance frequency, resonance amplitude and - 3 dB bandwidth.

3.1.1 Spherical particles

The radius of the spherical particles is varied from 325 to 425 nm, and the different resonance characteristics have

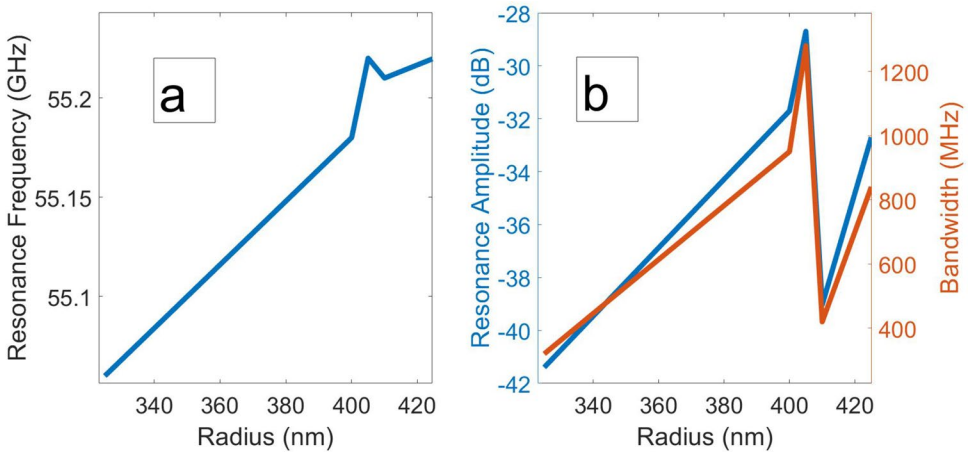

Fig. 5 Variation of **a** resonance frequency and **b** resonance amplitude and − 3 dB bandwidth with radius of spherical particles

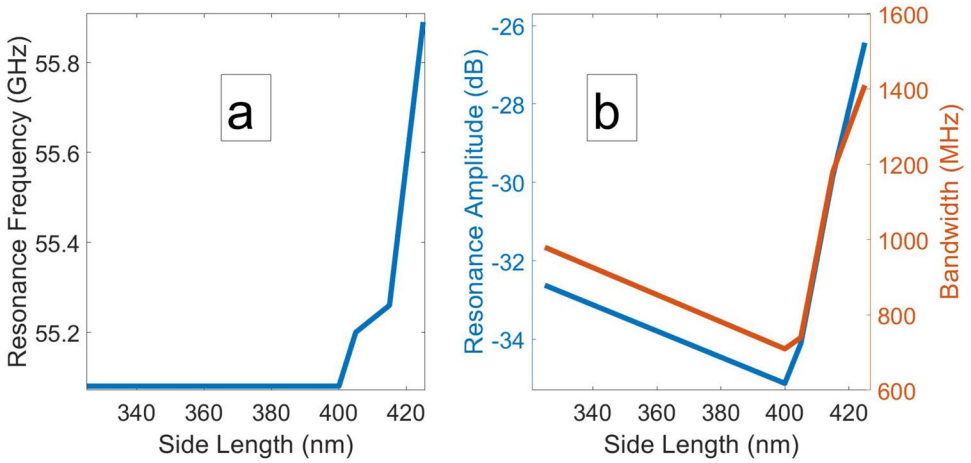

Fig. 6 Variation of **a** resonance frequency and **b** resonance amplitude and − 3 dB bandwidth with side length of cubical particles

been plotted in Fig. 5. From Fig. 5a, we see that as the radius of the spherical particles increases, the resonance frequency also increases. Further, the resonance amplitude and - 3 dB bandwidth show unique trends in specific regions. These trends depend upon the region of operation of the sensor and the sensor design. However, it is interesting to note that the resonance amplitude and the − 3 dB bandwidth vary in a similar fashion.

3.1.2 Cubical particles

For the cubical particles, the length of the side is varied from 325 to 425 nm. From Fig. 6 we observe that the resonance frequency increases with increasing side length. However, like in the case of spherical particles, the resonance amplitude and the − 3 dB bandwidth don't follow any general tendencies throughout the region of observation. While the behavior of the resonance frequency change is the same for both the spherical and cubical particles, the same can not be said for the other resonance characteristics. This could be attributed to the fact that volume plays a greater role in ascertaining the resonance frequency. However, the shape affects the other resonance characteristics more. It is also important to note that the resonance amplitude and the − 3 dB bandwidth follow the same trend.

3.1.3 Polyhedral particles

In this sub-section, polyhedral gold particles are taken and two different kinds of analyses are performed. Firstly, the number of sides of the polyhedral gold particles is varied. In the second case, for decahedral gold particles, the effects of the particle thickness variation is studied.

For a fixed radius of 300 nm and a fixed volume, the number of sides is varied from three to ten (Fig. 7). The results indicate that an increase in the number of sides when the volume is kept constant leads to a decrease in the resonance frequency. Furthermore, the resonance amplitude and bandwidth exhibit unique trends and don't vary evenly.

In the second part of the analysis, the height of decahedral particles is varied from 50 to 80 nm and the observations are shown in Fig. 8. The results suggest an increase in resonance

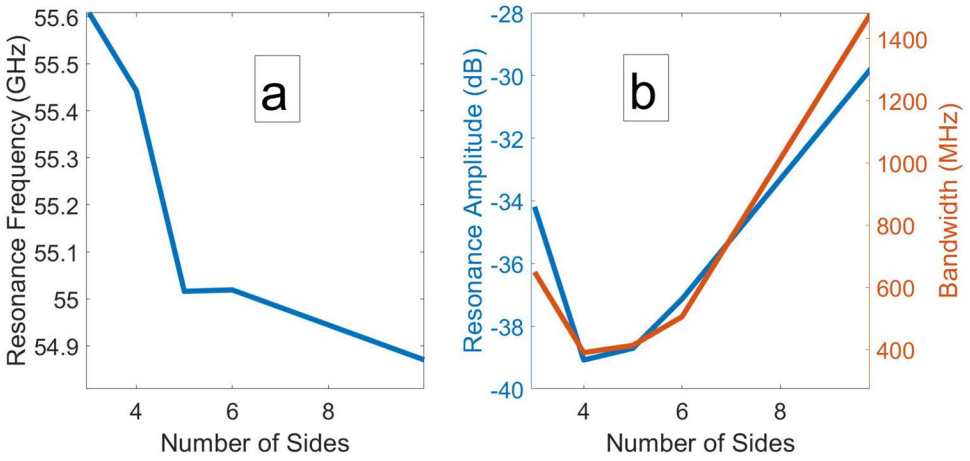

Fig. 7 Variation of **a** resonance frequency and **b** resonance amplitude and − 3 dB bandwidth with number of sides of polyhedral particles

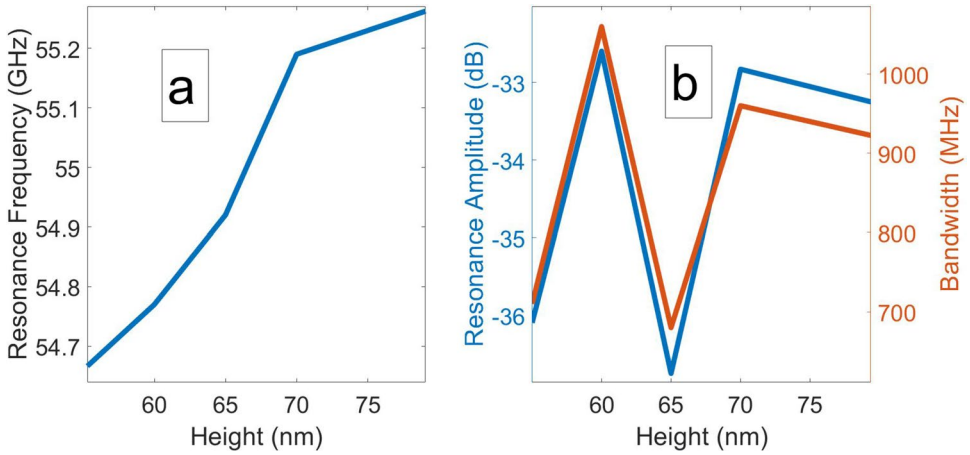

Fig. 8 Variation of **a** resonance frequency and **b** resonance amplitude and − 3 dB bandwidth with height of decahedral particles

frequency is associated with an increase in the height of the particles. Akin to the previous shapes studied, here also we observe that the resonance amplitude and the bandwidth follow specific trends which depend upon the sensor design and frequency of operation. However, the same behavior is exhibited by both the resonance amplitude as well as the bandwidth.

3.2 Simulation based study: relative arrangements of gold nanoparticles

Next, we have investigated the effects of relative arrangements of gold nanoparticles. We have analyzed a group of 30 particles of a given shape. For each shape, we have taken two sets of interparticle distances (say, clustered and non-clustered arrangements). We considered a height of 100 nm and a radius of 500 nm for the disc-shaped particles, spherical particles of a radius of 500 nm, and cubical particles of a side of length 500 nm. Various resonance characteristics are shown in Table 1.

Table 1 shows that there are no distinct indicators to segregate clustered arrangements from non-clustered arrangements. While for each of these cases, the response is unique and some specific trends can be noted, no general trends as such exist. For example, in the case of the spherical and the cylindrical systems, the resonance frequency of the non-clustered arrangements is higher. For the spherical and cubical systems, − 3 dB bandwidth is higher for the clustered system, while the resonance amplitude is lower for the non-clustered case.

3.3 Experimental verification

In order to verify the feasibility of performing such analysis, differentiation between gold particles with and without BSA coating is performed using the fabricated IDC resonating at 5 GHz. The samples are prepared according to the procedure mentioned in Sect. 2.2. The observed results for both the simulation as well as the experimental setup have been given in Table 2.

Table 2 suggests that gold particles coated with BSA exhibit characteristics different from that of the gold particles without any coating. For both the simulation as well as the experimental setup, the resonance frequency and the

Table 1 Variation of resonance frequency, resonance amplitude and − 3 dB bandwidth for clustered and non-clustered arrangements of gold nanoparticles

Shape	Cluster/non-cluster	Resonance frequency (in GHz)	S_{11} amplitude (in dB)	3 dB bandwidth (in MHz)
Spherical	Non-Clustered	55.5	− 33.64732946	790
	Clustered	54.94	− 30.60285058	1180
Disc-shaped	Non-clustered	55.01	− 34.71717347	780
	Clustered	54.91	− 36.79238049	600
Cubical	Non-clustered	55.11	− 35.75759243	660
	Clustered	55.44	− 34.21228526	710

Table 2 Variation of resonance frequency, resonance amplitude and − 3 dB bandwidth for coated and non-coated gold nanoparticles

Sample	Setup	Resonance frequency (in GHz)	S_{11} amplitude (in dB)	− 3 dB bandwidth (in MHz)
Only gold	Simulation	54.66	− 36.06028843	690
	Experimental	3.60	− 31.77901799	60
BSA coated gold	Simulation	54.61	− 40.17725627	470
	Experimental	3.48	− 40.75466597	60

resonance amplitude of the biolayer-coated gold particles are lower than that of the uncoated ones. The bandwidth, on the other hand, remains constant for the experimental setup, while for the simulation in HFSS, we observe a decrease in bandwidth with the coating of gold particles.

3.4 Discussion

The IDC-based RF sensor's resonance characteristics loaded with gold particles depend upon several aspects. It includes the position of the particles, the volume, the morphological features such as radius, thickness, shape and the relative arrangement of particles. It also depends upon the interaction between the gold particles. The response generated is an amalgamation of the effects of these different factors. In most cases, some factors are dominant. It is also possible to have instances where the change in the various factors are comparable. The net effect, in that case, could result in a dramatic change in the resonance characteristics. It could also involve no change in the characteristics, with the effects nullifying each other. Furthermore, a different parameter might become dominant under certain conditions and generate unexpected outcomes.

In our work, we have studied the variation of morphological features of gold particles along with their varying arrangements. In particular, in the first half, we studied the effect of changing: (a) the radius of cubical and spherical particles and (b) the height of polyhedral particles. The increase in the radius and height results in an effective increase in the size of the particles. The results showed that for all three cases, this increase in size, in turn, increases the resonance frequency. Further, in the case of the radius variation of cubical particles and spherical particles, no definite trends are followed by the resonance amplitude and bandwidth. Instead, these results suggest that the trends are frequency dependent.

From Karkkainen et al. (2000), we know that the effective permittivity of a mixture of cylindrical particles of permittivity, ϵ_i and volume fraction, f, dispersed in a material of permittivity, ϵ_e , is given by

$$\epsilon_{f,max} = f\epsilon_i + (1-f)\epsilon_e \tag{2}$$

$$\epsilon_{f,min} = \epsilon_i\epsilon_e / f\epsilon_i + (1-f)\epsilon_e \tag{3}$$

The equation above indicates that if $\epsilon_e > \epsilon_i$, the effective permittivity decreases as the volume fraction f increases.

Also, for a microstrip-based structure (Rano et al. 2020) if the effective permittivity of the supersubstrate decreases, the net permittivity of the sensor drops. This, in turn, leads to an increase in the resonance frequency.

The increase in radius or height leads to an increase in the volume fraction of the gold particles. This, in turn, decreases the effective permittivity of the solution of gold particles in water, as indicated by (1). The water layer acts as the supersubstrate and as its permittivity drops, the effective permittivity of the antenna also decreases. As a result, the resonance frequency, as dictated by (2) and (3), increases.

The resonance amplitude and the bandwidth are related parameters, as exhibited by the trends observed throughout the analysis. For all cases under study, the amplitude and bandwidth variation is synchronized. This could be

attributed to the effect of the effective resistance offered by these particles that affect the Q-factor of the sensor and, in turn, affects the sensor's bandwidth. However, these two parameters do not follow well-defined, consistent trends. They vary in different ways in different regions. Also, the trends differ for different shapes under study. This suggests that such parameters are system and conditions dependent. It is also important to note that these trends are frequency and sensor design dependent.

As part of the morphological variation, we also looked at the change in the number of sides of polyhedral particles. In order to keep the volume constant, we have changed the height of the particles while keeping the circumradius constant. We observed that the resonance frequency increases with an increase in the number of sides. This observation can be understood based on the corner effect. The larger the number of sides of the polyhedral particle, the more would be the number of sharp corners. It would result in a greater density of E-field in those pockets. This would essentially lead to greater shifts from the sensor's resonance frequency in unloaded conditions, and the observations in this work suggest the same.

In the last part of our analysis, we looked at clustered and non-clustered systems. We observed that no significant identifiers exist that can enable simplified identification of these systems. The absence of clear demarcation between clustered and non-clustered systems could be attributed to the simultaneous change of various parameters. For instance, both the position of the gold particles and the interaction between the particles vary. Since the E-field on the surface of the IDC is not uniform, a change of position could lead to varying results. The distances between the particles do not vary systematically in these cases. As a result, the interaction between the particles changes due to their specific arrangements. Furthermore, the volume remains constant. All of these things together contribute to the absence of any trend in the results obtained.

The feasibility of performing particle size estimation using RF sensing was first performed in Zarifi et al. (2016). The authors demonstrated samples containing varied sizes of particles possess unique dielectric properties. These properties,in turn, give rise to distinct RF signatures. However, the particle size was restricted to 40–400 µm. This work explores particle size at a much smaller scale and focuses on the individual morphology variation. Additionally, it looks at the variation of arrangements of particles. Further, in Abdolrazzaghi et al. (2017, 2016), such analyses was carried out asphaltene particles. Nanoparticles, particularly plasmonic nanoparticles like gold, were not studied previously.

More in-depth studies involving the effects of sample's volume, position, etc., are required for a comprehensive understanding of such cases. The findings show that resonance frequency can detect the variation in the size and morphological parameters of the gold nanoparticles. The resonance amplitude and − 3 dB bandwidth results depend on the systems studied. It suggests that these two parameters need to be used in conjugation with the resonance frequency for differentiating the gold nanoparticles.

4 Conclusion

RF-based differentiation of nanoparticles can be beneficial in various studies and applications. This work investigated the possibility of using Radio Frequency based sensing for analysis of variation of morphological features of gold nanoparticles. Spherical, cubical, and polyhedral particles in aqueous media were studied as samples. The variation of different particle parameters like the radius, thickness, number of sides, and the relative arrangements of the gold nanoparticles have been investigated. The findings suggest that the resonance frequency, along with the resonance amplitude and − 3 dB bandwidth, may be used to detect the variation in the size, morphological parameters, and relative arrangements of the gold nanoparticles. However, more in-depth studies will be helpful to understand the effects more clearly and establishing general principles regarding it.

Acknowledgements This work was supported by the Department of Biotechnology (DBT), Govt.of India, as a part of the project, "Design of Radio Frequency Cavities for Detection of Specific Protein" (DBT-Ref no. BT/PR20720/MED/32/590/2017). A.M thanks IHub-Data, IIIT Hyderabad for a research fellowship.

Author contributions AM, SA, TS and PB discussed the ideas and planned the simulations. AM performed the simulations and experiments, and wrote the manuscript. SA, TS and PB helped AM in reviewing and editing the manuscript.

Declarations

Conflict of interest The authors declare no conflict of interest.

References

Abdolrazzaghi M, Zarifi MH, Floquet CF, Daneshmand M (2017) Contactless asphaltene detection using an active planar microwave resonator sensor. Energy Fuels 31(8):8784–8791

Abdolrazzaghi M, Zarifi MH, Daneshmand M, Floquet CF (2016) Contactless asphaltene solid particle deposition monitoring using active microwave resonators. IEEE Sens 1–3

Baetke SC, Lammers T, Kiessling F (2015) Applications of nanoparticles for diagnosis and therapy of cancer. Br J Radiol 88(1054):20150207

Bahar A, Zakaria Z, Arshad M, Isa A, Dasril Y, Alahnomi R (2019) Real time microwave biochemical sensor based on circular SIW approach for aqueous dielectric detection. Sci Rep 9(1):1–12

Booth NJ, ad Orloff C, Mateu J, Janezic M, Rinehart M, Beall J (2010) Quantitative permittivity measurements of nanoliter liquid volumes in microfluidic channels to 40 GHz. IEEE Trans Instrum Meas 59(12):3279–3288

Boybay MS, Ramahi OM (2012) Material characterization using complementary split-ring resonators. IEEE Trans Instrum Meas 61(11):3039–3046

Chang C-C, Lee C-H, Wu T-H, Chen C-P, Chen C-Y, Lin C-W (2017) Reversion of gold nanoparticle aggregates for the detection of cu 2+ and its application in immunoassays. Analyst 142(24):4684–4690

Chen Y-F, Wu H-W, Hong Y-H, Lee H-Y (2014) 40 ghz rf biosensor based on microwave coplanar waveguide transmission line for cancer cells (hepg2) dielectric characterization. Biosens Bioelectron 61:417–421

Dalmay C, Leroy J, Pothier A, Blondy P (2014) Development of high frequency microfluidic biosensors for intracellular analysis. Proc Eng 87:54–57

Daniel M-C, Astruc D (2004) Gold nanoparticles: assembly, supramolecular chemistry, quantum-size-related properties, and applications toward biology, catalysis, and nanotechnology. Chem Rev 104(1):293–346

De M, Ghosh PS, Rotello VM (2008) Applications of nanoparticles in biology. Adv Mater 20(22):4225–4241

Dondapati SK, Sau TK, Hrelescu C, Klar TA, Stefani FD, Feldmann J (2010) Label-free biosensing based on single gold nanostars as plasmonic transducers. ACS Nano 4(11):6318–6322

Elsheakh D, Elsadek H, Abdullah E, Atteya S, Elmazny W (2013) Novel rapid detection of different viruses in blood using microimmuno-sensor. In: 2013 7th European Conference on Antennas and Propagation (EuCAP). IEEE, pp 1128–1131

Facer G, Notterman D, Sohn L (2001) Dielectric spectroscopy for bioanalysis: from 40 Hz to 26.5 GHz in a microfabricated wave guide. Appl Phys Lett 78(7):996–998

Grenier K, Dubuc D, Poleni P, Kumemura M, Toshiyoshi H, Fujii T, Fujita H (2010) Resonant based microwave biosensor for biological cells discrimination. In: IEEE Radio and Wireless Symposium (RWS). IEEE 2010, pp 523–526

Grzelczak M, Pérez-Juste J, Mulvaney P, Liz-Marzán LM (2008) Shape control in gold nanoparticle synthesis. Chem Soc Rev 37(9):1783–1791

Haes AJ, Hall WP, Chang L, Klein WL, Van Duyne RP (2004) A localized surface plasmon resonance biosensor: First steps toward an assay for alzheimer's disease. Nano Lett 4(6):1029–1034

Han X, Xu K, Taratula O, Farsad K (2019) Applications of nanoparticles in biomedical imaging. Nanoscale 11(3):799–819

Hong Y, Huh Y-M, Yoon DS, Yang J (2012) Nanobiosensors based on localized surface plasmon resonance for biomarker detection. J Nanomater

Jana NR, Gearheart L, Murphy CJ (2001) Seed-mediated growth approach for shape-controlled synthesis of spheroidal and rod-like gold nanoparticles using a surfactant template. Adv Mater 13(18):1389–1393

Jang Y-H, Lee K-N, Kim Y-K (2006) Characterization of a single-crystal silicon micromirror array for maskless uv lithography in biochip applications. J Micromech Microeng 16(11):2360

Karkkainen K, Sihvola A, Nikoskinen K (2000) Effective permittivity of mixtures: numerical validation by the fdtd method. IEEE Trans Geosci Remote Sens 38(3):1303–1308

Kim JW (2008) Development of interdigitated capacitor sensors for direct and wireless measurements of the dielectric properties of liquids

Kim J, Babajanyan A, Hovsepyan A, Lee K, Friedman B (2008) Microwave dielectric resonator biosensor for aqueous glucose solution. Rev Sci Instrum 79(8):086107

Lee H, Yook J (2014) Recent research trends of radio-frequency biosensors for biomolecular detection. Biosens Bioelectron 61:448–459

Lee H, Lee J, Moon H, Jang I, Choi J, Yook J, Jung H (2012) A planar split-ring resonator-based microwave biosensor for label-free detection of biomolecules. Sens Actuators B Chem 169:26–31

Liu G, Zhang R, Li L, Huang X, Li T, Lu M, Xu D, Wang J (2018) Anti-agglomeration behavior and sensing assay of chlorsulfuron based on acetamiprid-gold nanoparticles. Nanomaterials 8(7):499

Mateu J, Orloff N, Rinehart M, Booth J (2007) Broadband permittivity of liquids extracted from transmission line measurements of microfluidic channels. In: IEEE/MTT-S international microwave symposium. IEEE 2007, pp 523–526

Mazumder A, Azeemuddin S, Sau TK, Bhimalapuram P (2020b) Role of shape of gold nanoparticles in sensing biomolecules using radio-frequency based sensors. IEEE Sens 1–4

Mazumder A, Azeemuddin S, Sau T. K, Bhimalapuram P (2020a) Study of gold particles in HFSS with varying physical parameters and arrangements. In: 2020 IEEE 15th international conference on nano/micro engineered and molecular system (NEMS), pp 529–532

Mehrotra P, Chatterjee B, Sen S (2019) EM-wave biosensors: a review of RF, microwave, mm-wave and optical sensing. Sensors 19(5):1013

Mohammadi S, Wiltshire B, Jain MC, Nadaraja AV, Clements A, Golovin K, Roberts DJ, Johnson T, Foulds I, Zarifi MH (2020) Gold coplanar waveguide resonator integrated with a microfluidic channel for aqueous dielectric detection. IEEE Sens J 20(17):9825–9833

Narang R, Mohammadi S, Ashani M, Sadabadi H, Hejazi H, Zarifi M, Sanati-Nezhad A (2018) Sensitive, real-time and non-intrusive detection of concentration and growth of pathogenic bacteria using microfluidic-microwave ring resonator biosensor. Sci Rep 8(1):1–10

Nee Haase N, Fuge T, G, AHK, Zeng, Jacob A (2015) Miniaturized transmission-line sensor for broadband dielectric characterization of biological liquids and cell suspensions. IEEE Trans Microw Theory Tech 63(10):3026–3033

Nikolic-Jaric M, Romanuik S, Ferrier G, Bridges G, Butler M, Sunley K, Thomson D, Freeman M (2009) Microwave frequency sensor for detection of biological cells in microfluidic channels. Biomicrofluidics 3(3):034103

Ocket I, Song L, Grillet D, Embrechts B, Schreurs D, De Raedt W, Nauwelaers B (2013) Dielectric characterization of biological liquids and tissues up to 110 GHz using an LTCC CPW sensor. In: 2013 IEEE topical conference on biomedical wireless technologies, networks, and sensing systems. IEEE, pp 43–45

Peyman A, Kos B, Djokic M, Trotovsek B, Limbaeck Stokin C, Sersa G, Miklavcic D (2015) Variation in dielectric properties due to pathological changes in human liver. Bioelectromagnetics 36(8):603–612

Porwal P, Syed A, Bhimalapuram P, Sau TK (2016) Detection of biotin-streptavidin interaction using rf interdigitated capacitive cavity. In: IEEE MTT-S International Microwave and RF Conference (IMaRC), pp 1–4

Rano D, Chaudhary MA, Hashmi MS (2020) A new model to determine effective permittivity and resonant frequency of patch antenna covered with multiple dielectric layers. IEEE Access 8:418–430

Rotello V (2004) Nanoparticles: building blocks for nanotechnology. Springer

RoyChoudhury S, Rawat V, Jalal A, Kale S, Bhansali S (2016) Recent advances in metamaterial split-ring-resonator circuits as biosensors and therapeutic agents. Biosens Bioelectron 86:595–608

Rukavina AV (2015) Non-invasive liquid recognition based on interdigital capacitor. Sens Actuators A 228:145–150

Sau TK, Murphy CJ (2004) Room temperature, high-yield synthesis of multiple shapes of gold nanoparticles in aqueous solution. J Am Chem Soc 126(28):8648–8649

Schmid G (2011) Nanoparticles: from theory to application. Wiley

Shete M, Shaji M, Akhtar MJ (2013) Design of a coplanar sensor for rf characterization of thin dielectric samples. IEEE Sens J 13(12):4706–4715

Song C, Azimuudin S, Lee B, Harackiewicz F, Yen M, Ralu D, Hoffman A, Wang P (2006) Microwave dielectric properties of on-chip liquid films. In: IEEE/NLM life science systems and applications workshop. IEEE, pp 1–2

Su J, Zhou Z, Li H, Liu S (2014) Quantitative detection of human chorionic gonadotropin antigen via immunogold chromatographic test strips. Anal Methods 6(2):450–455

Surowiec A, Stuchly S, Barr J, Swarup A (1988) Dielectric properties of breast carcinoma and the surrounding tissues. IEEE Trans Biomed Eng 35(4):257–263

Velez P, Su L, Grenier K, Mata-Contreras J, Dubuc D, Martin F (2017) Microwave microfluidic sensor based on a microstrip splitter/combiner configuration and split ring resonators (srrs) for dielectric characterization of liquids. IEEE Sens J 17(20):6589–6598

Wang Y, Yang F, Yang X (2010) Colorimetric detection of mercury (ii) ion using unmodified silver nanoparticles and mercury-specific oligonucleotides. ACS Appl Mater Interfaces 2(2):339–342

Wang F, Lu Y, Yang J, Chen Y, Jing W, He L, Liu Y (2017) A smartphone readable colorimetric sensing platform for rapid multiple protein detection. Analyst 142(17):3177–3182

Wang F, Sun J, Lu Y, Zhang X, Song P, Liu Y (2018) Dispersion-aggregation-dispersion colorimetric detection for mercury ions based on an assembly of gold nanoparticles and carbon nanodots. Analyst 143(19):4741–4746

Wu H (2016) Label-free and antibody-free wideband microwave biosensor for identifying the cancer cells. IEEE Trans Microw Theory Tech 64(3):982–990

Wu B, Zou F, Wang X, Koh K, Wang K, Chen H (2017) The colorimetric assay of diamine oxidase activity with high sensitivity based on calixarene derivative-capped gold nanoparticles. Anal Methods 9(14):2153–2158

Xu K (2021) Silicon electro-optic micro-modulator fabricated in standard cmos technology as components for all silicon monolithic integrated optoelectronic systems. J Micromech Microeng 31(5):054001

Xu K, Chen Y, Okhai TA, Snyman LW (2019) Micro optical sensors based on avalanching silicon light-emitting devices monolithically integrated on chips. Opt Mater Exp 9(10):3985–3997

Yue G, Su S, Li N, Shuai M, Lai X, Astruc D, Zhao P (2016) Gold nanoparticles as sensors in the colorimetric and fluorescence detection of chemical warfare agents. Coord Chem Rev 311:75–84

Zarifi MH, Shariaty P, Abdolrazzaghi M, Hashisho Z, Daneshmand M (2016) Particle size characterization using a high resolution planar resonator sensor in a lossy medium. Sens Actuators, B Chem 234:332–337

Zazo H, Colino CI, Lanao JM (2016) Current applications of nanoparticles in infectious diseases. J Control Rel 224:86–102

Zhang L, Du Puch C, Lacroix A, Dalmay C, Pothier A, Lautrette C, Battu S, Lalloue F, Jauberteau M, Blondy P (2012) Microwave biosensors for identifying cancer cell aggressiveness grade. In: IEEE/MTT-S International Microwave Symposium Digest. IEEE 2012, pp 1–3

Zou L, Shen R, Ling L, Li G (2018) Sensitive dna detection by polymerase chain reaction with gold nanoparticles. Anal Chim Acta 1038:105–111